Provided for non-commercial research and education use.
Not for reproduction, distribution or commercial use.

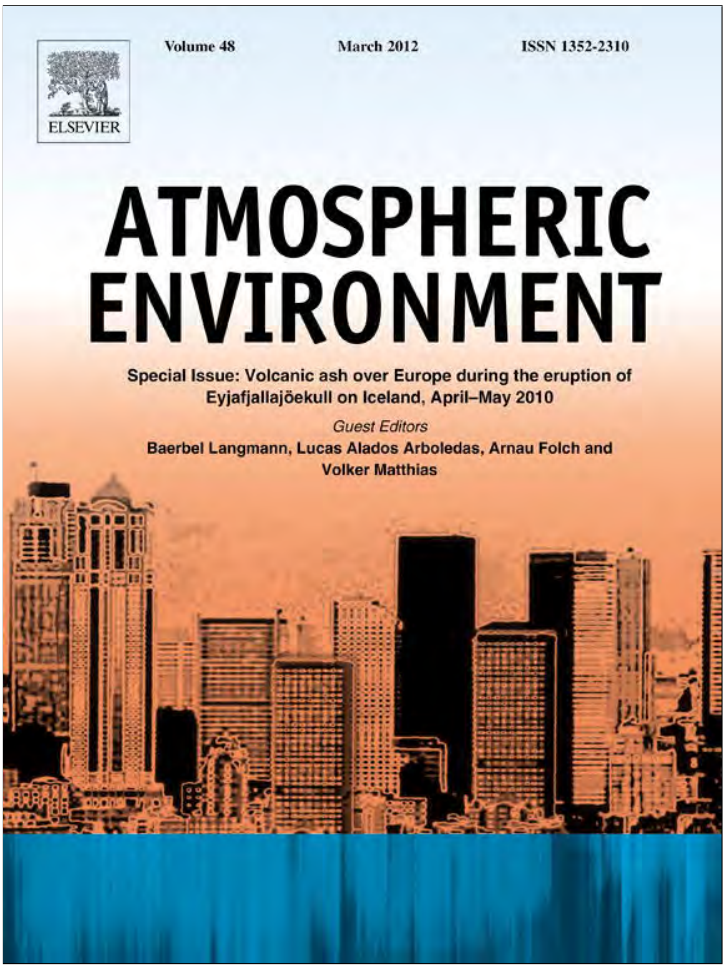

This article appeared in a journal published by Elsevier. The attached copy is furnished to the author for internal non-commercial research and education use, including for instruction at the authors institution and sharing with colleagues.

Other uses, including reproduction and distribution, or selling or licensing copies, or posting to personal, institutional or third party websites are prohibited.

In most cases authors are permitted to post their version of the article (e.g. in Word or Tex form) to their personal website or institutional repository. Authors requiring further information regarding Elsevier's archiving and manuscript policies are encouraged to visit:

http://www.elsevier.com/copyright

Author's personal copy

Atmospheric Environment 48 (2012) 195–204

Contents lists available at ScienceDirect

Atmospheric Environment

journal homepage: www.elsevier.com/locate/atmosenv

Simulations of the 2010 Eyjafjallajökull volcanic ash dispersal over Europe using COSMO–MUSCAT

Bernd Heinold [a,*], Ina Tegen [a], Ralf Wolke [a], Albert Ansmann [a], Ina Mattis [a], Andreas Minikin [b], Ulrich Schumann [b], Bernadett Weinzierl [b]

[a] Leibniz Institute for Tropospheric Research, 04318 Leipzig, Germany
[b] Deutsches Zentrum für Luft- und Raumfahrt (DLR), Institut für Physik der Atmosphäre, 82234 Oberpfaffenhofen, Germany

ARTICLE INFO

Article history:
Received 2 February 2011
Received in revised form
4 May 2011
Accepted 5 May 2011

Keywords:
Volcanic ash plume
Eyjafjallajökull
Aerosol transport modelling
COSMO–MUSCAT model

ABSTRACT

The ash plume of the Icelandic volcano Eyjafjallajökull covering Europe in April and May 2010 has notably attracted the interest of atmospheric researchers. Emission, transport, and deposition of the volcanic ash are simulated with the regional chemistry-transport model COSMO–MUSCAT. Key input parameters for transport models are the ash injection height, which controls the ash layer height during long-range transport, and the initial particle size distribution, which influences the sedimentation velocity. For each model layer, relative release rates are parameterised using stereo-derived plume heights from NASA's space-borne Multi-angle Imaging SpectroRadiometer (MISR) observations near the source. With this model setup the ash is emitted at several levels beneath the maximum plume heights reported by the Volcanic Ash Advisory Centre (VAAC) London. The initial particle size distribution used in COSMO–MUSCAT is derived from airborne in-situ measurements. In addition, the impact of different injection heights on the vertical distribution of the volcanic ash plume over Europe is shown. Ash emissions at specific control levels allow to assess the relative contribution of each layer to the spatial distribution after transport. The model results are compared to aerosol optical depths from European Sun photometer sites, lidar profiles measured over Leipzig/Germany, and ground-based microphysical measurements from several German air quality stations. In particular the good agreement between modelled vertical profiles of volcanic ash and lidar observations indicates that using the MISR stereo-height retrievals to characterize atmospheric ash input provide an alternative to injection height models in case of lacking information on eruption dynamics.

Crown Copyright © 2011 Published by Elsevier Ltd. All rights reserved.

1. Introduction

During the continuing eruption of the Eyjafjallajökull volcano in April and May 2010, the volcanic ash plume severely disrupted air traffic in Europe. The Volcanic Ash Advisory Centre (VAAC) in London provided ash dispersal simulations with the NAME III model (Jones et al., 2007). The Lagrangian model forecasted the ash plume location, and warning was issued for regions where presence of volcanic ash was expected. Those predictions led to the exceptional decision to close large parts of the European air space, which, according to EUROCONTROL, caused more than 100,000 flight cancellations in the first week after the eruption (Schumann et al., 2011).

Volcanic ash is considered to be harmful for aircraft engines due to its low melting point (Miller and Casadevall, 2000), which is below the engine operating temperature (>1000 °C) and lower than the melting point of, e.g., Saharan dust. Volcanic ash may melt and clog the interior of the jet engine, whereas desert dust may be sucked through without being melted, which poses less risk to aircraft (Casadevall, 1994). Aircraft are often operated without major problems in regions with elevated particle mass concentrations, e.g., in the vicinity of the Sahara desert (Weinzierl et al., 2009). Safety limits were established, determining that ash concentrations lower than 0.2 mg m^{-3} pose no risk for air traffic; and with ash concentrations larger than 2 mg m^{-3} air traffic is not allowed. At the end of the eruption, the limit of the no-fly zone was increased to 4 mg m^{-3}. These higher limits could have led to a smaller impact on air traffic compared to closing the air space at any ash concentration. However, quantitative forecasts of ash concentration are problematic due to unknown emission

* Corresponding author. Present address: School of Earth & Environment, University of Leeds, Leeds LS2 9JT, United Kingdom.
E-mail address: b.heinold@leeds.ac.uk (B. Heinold).

1352-2310/$ – see front matter Crown Copyright © 2011 Published by Elsevier Ltd. All rights reserved.
doi:10.1016/j.atmosenv.2011.05.021

Author's personal copy

parameters (i.e., mass eruption rate, injection height, vertical distribution of ash release and particle size distribution).

Given the large economic impact of the closure of air space, the transport models used for forecasting ash distributions should strive to obtain authoritative quantitative results for the 3-D distribution of the particle concentrations. While uncertainties in ash production, size spectrum and injection height were causing lack of quantification in the model forecasts, many data are now available from various different observations that allow evaluation of the ash particle transport in the volcanic plume in transport models. This will lead to improvements of the model and ultimately improve of ash concentration forecasting during possible future events. Here we present results of the simulations of the Eyjafjallajökull volcano ash plume by a regional aerosol transport model over the European domain, together with model evaluation by sun photometer and lidar data as well as particle concentration measured at selected ground stations.

2. The 2010 Eyjafjallajökull volcano eruption

On 14 April 2010 the eruption of Eyjafjallajökull volcano (63.63°N, 19.62°W, 1666 m asl) on Iceland started to send a vast ash plume into the troposphere. The eruption can be classified as mid-sized eruption or as a 4 on the Volcanic Explosivity Index [http://www.smithsonianmag.com/science-nature/91838474.html]. The explosive eruption occurred beneath a glacial ice cap, which caused in the first days flooding from the melting ice (Gudmunsson et al., 2010). The cold melt water mixed with the rising magma and quenched it. As a result, strongly fragmented glassy ash particles were formed, which were carried toward Central Europe by the prevailing wind system.

During the three following days strong ash production continued, decreasing by 19 April (Gudmunsson et al., 2010). Around 1 May the explosive volcanic activity increased again, together with increasing ash production. On the first day of the eruption the plume height reached more than 9 km, decreasing during the following days. A high-pressure system over Iceland and later Scandinavia favoured north-westerly winds transporting the ash to Central Europe within 1–2 days after the start of the eruption. The plume crossed large parts of Europe, reaching Germany at heights between 2 and 7 km altitude. It started to subside on 16 April and was mixed into the planetary boundary layer on 17 April (Flentje et al., 2010). In central Europe the volcanic ash could be identified in ground-based lidar measurements (Ansmann et al., 2010), elevated particle concentrations from air quality stations (Flentje et al., 2010) and aircraft measurements (Schumann et al., 2011). Optical depths, as picked up by the Aerosol Robotic Network (AERONET), reached values up to 1 at 500 nm (Ansmann et al., 2010).

3. Method

3.1. Model description and setup

The transport simulations for the Eyjafjallajökull eruption are performed using COSMO–MUSCAT. The regional model system consists of the non-hydrostatic model COSMO (Steppeler et al., 2003) as meteorological driver, and the online-coupled 3-D chemistry tracer transport model MUltiScale Chemistry Aerosol Transport Model (MUSCAT) (Wolke et al., 2004; Renner and Wolke, 2010). In MUSCAT, microphysical processes and chemical reactions are described by time-dependent mass balance equations. The advection of chemical species and aerosols is computed by a third-order upstream scheme and an implicit-explicit scheme is applied for temporal integration (Wolke and Knoth, 2000). Transport and deposition of aerosol particles are simulated using meteorological and hydrological fields from COSMO updated every advection time step. Volcanic ash transport is simulated with a COSMO–MUSCAT version that was originally developed for Saharan dust simulations (Heinold et al., 2007, 2009). It accounts for the spatial–temporal evolution of the size distribution of volcanic ash particles. The modelled volcanic ash is transported as passive tracer in five independent size classes with radius limits at 0.1 μm, 0.3 μm, 0.9 μm, 2.6 μm, 8 μm and 24 μm. Larger ash particles are quickly removed by sedimentation near the volcano, and thus not considered for long-range transport.

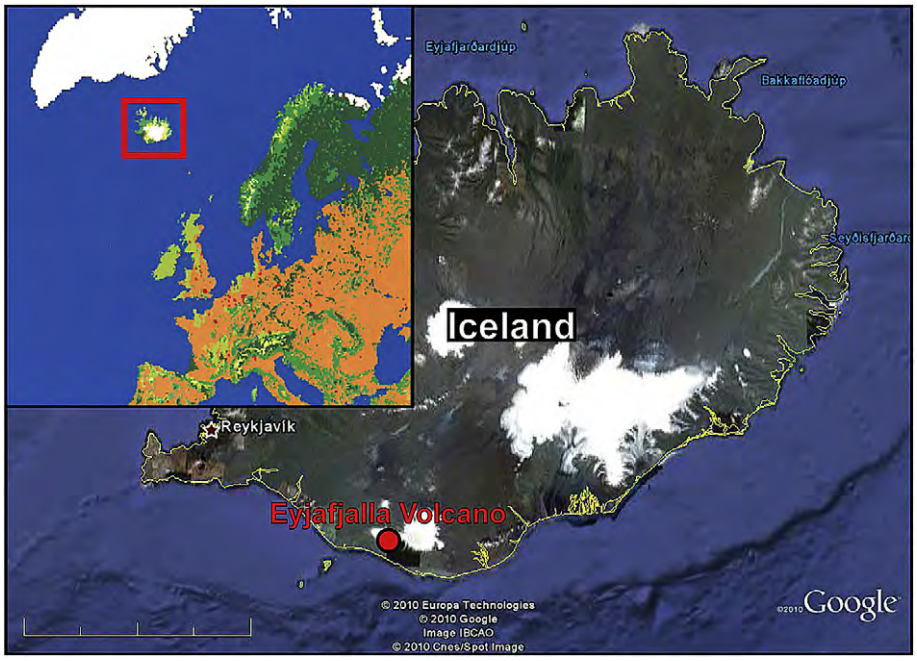

Fig. 1. Map of Iceland with the location of the Eyjafjallajökull volcano (63.63°N, 19.62°W, 1666 m asl) (Source: Google Earth, 2010). The top-left inset shows the model domain.

Author's personal copy

Volcanic emissions are treated as vertical line source above the Eyjafjallajökull crater. Particle release rates are taken from the Unified EMEP model simulations conducted by The Norwegian Meteorological Institute [https://wiki.met.no/emep/emep_volcano_plume]. They provide emission rates for primary particulate matter of diameter smaller than 10 μm (PM10), which base on first estimates on tephra volume and magma effusion rates for the first 72 h (14–16 April 2010) of the eruption. The values were obtained from field measurements by volcanologists from the University of Iceland. The initial particle size distribution used in COSMO–MUSCAT is derived from in-situ measurements aboard the Falcon aircraft of the German Aerospace Centre (Deutsches Zentrum für Luft- und Raumfahrt, DLR). The particle sizes were taken within the volcanic ash layer over Leipzig/Germany at about 4.3 km height on 19 April 2010 (Schumann et al., 2011). Assuming that the shape of size distribution for diameters smaller than 15 μm does not change significantly during transport while larger particles deposit rapidly near the source, mass fractions of the initial particle size distribution are computed by fitting the model values to the observations. The mass fractions for particles larger than 15 μm are obtained by extrapolation of the measured size distribution (Fig. 2, bottom panel). Then, the given PM10 emissions (Table 1) are distributed over the model size bins accordingly. The emission rates are assumed to be constant throughout each day. The volcanic ash is released at six model layers below the maximum plume height based on London VAAC reports (see Table 1 for the injection height range). The MISR plume height project [http://misr.jpl.nasa.gov] provides statistical information on the vertical extent of the ash plume for several days in April and May 2010 (Fig. 3). The stereo-height product, with about 500-m accuracy, is suitable to describe injection heights for transport modelling (Kahn et al., 2007; Scollo et al., 2010). Frequency distributions of the plume height near Eyjafjallajökull are used to estimate fractional emission rates for each model layer. As an example, Table 2 lists the vertical mass distribution factors for the injection heights on 19 April. Although emission rate and injection height are linked, fixed average mass fractions are applied throughout the model run independently of the plume top height, as the MISR products do not cover the entire period. More than one-third of the material is emitted at the median height, which is on average about 0.7 of the maximum plume height. In addition to the standard case, the uncertainties in the modelled volcanic ash distribution due to the choice of injection heights are studied. Additional independent particle tracers are released in each 3 model layers below (later referred to as “Low”), within (“Medium”) and above (“High”) the standard emission height range (“MISR”). The tracer species are transported separately by the prevailing wind in the respective atmospheric layers. Tracking their dispersion and comparisons of the model results to observations indicate to which extent different injection heights contribute to the actual spatial-temporal evolution of the Eyjafjallajökull ash plume.

Table 1
Primary ash particle (PM10) release rate as provided by the Norwegian Meteorological Institute and range of injection height. Plume top heights are based on London VAAC reports. The value in parentheses is the height of maximum emission, which relates to the median plume height as observed by MISR satellite.

Date	PM10 [kg s^{-1}]	Injection height (median) [km]
14/04/2010	1000	4.5–7.6 (5.6)
15/04/2010–16/04/2010	5000	4.5–7.6 (5.6)
17/04/2010	9000	4.5–7.6 (5.6)
18/04/2010	2000	2.0–4.1 (2.7)
19/04/2010	7000	1.5–3.3 (2.1)
20/04/2010	300	1.5–3.3 (2.1)
21/04/2010–02/05/2010	300	2.0–4.1 (2.7)
03/05/2010–04/05/2010	2000	2.0–4.1 (2.7)
05/05/2010	2000	3.3–5.9 (4.2)
06/05/2010–09/05/2010	2000	4.1–7.0 (5.2)
10/05/2010–20/05/2010	2000	2.6–4.9 (3.5)
21/05/2010–22/05/2010	100	2.6–4.9 (3.5)
23/05/2010	0	2.6–4.9 (3.5)
24/05/2010– today	0	2.6–4.9 (3.5)

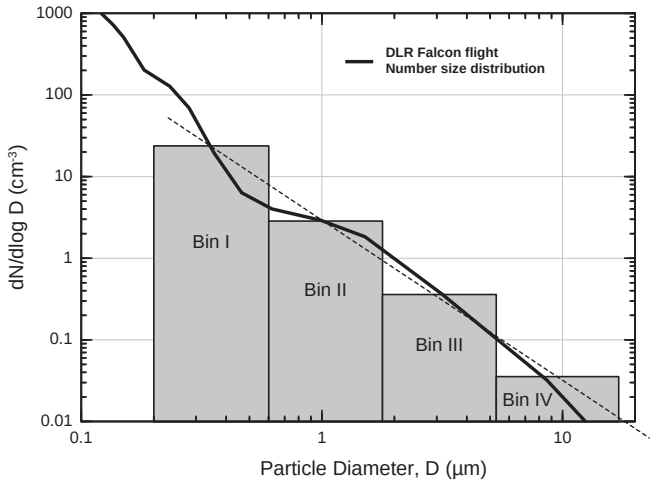

Initial ash particle size distribution

Bin n	Radii	Mass fraction	
Bin I	0.1 - 0.3 μm	0.4 %	100 % EMEP PM10 emissions
Bin II	0.3 - 0.9 μm	1.4 %	
Bin III	0.9 - 2.6 μm	11.9 %	
Bin IV	2.6 - 7.9 μm	19.7 %	
Bin V	7.9 - 24. μm	66.6 %	

Fig. 2. Number size distribution from airborne measurements aboard Falcon aircraft within the ash layer over Leipzig at about 4.3 km height on 19 April 2010. Grey-shaded bars indicate the initial size distribution used in the model, which was fitted to the measured values. The table (bottom panel) compiles mass fractions in percentage of the initial ash particle size distribution. (For interpretation of the references to colour in this figure legend, the reader is referred to the web version of this article.)

The volcanic ash particles are removed from the atmosphere by dry and wet deposition processes. Dry deposition is due to gravitational settling and turbulent mixing. Wet deposition means the particle removal by precipitation including the scavenging of ash particles by droplets or ice crystals within (rain-out) and below the cloud (wash-out). Dry deposition is usually most relevant for ash particles larger than 5 μm near the volcano, while wet deposition dominates the removal of submicrometer-sized particles during long-range transport. Dry deposition is computed following Seinfeld and Pandis (1998). The parameterization of wet deposition follows Berge (1997) and takes size-resolved scavenging ratios into account. However, since no substantial precipitation events occurred in the April–May 2010 period, the dry removal processes were most important in this case.

For the volcanic eruption simulations a horizontal grid resolution of 28 km is used. Fig. 1 shows the model domain and the location of Eyjafjallajökull. The model has 40 vertical layers with the lowest layer extending to a depth of 68 m. The modelled time period covers the days from 14 April to 24 May 2010. Initialization and large-scale meteorological forcing of COSMO–MUSCAT are based on 6-h re-analysis data from the German weather service (DWD – Deutscher Wetterdienst) global model GME. The model is reinitialized every 48 h to avoid long-term drifts in modelled meteorological fields. The first cycle starts with zero initial aerosol concentrations; following cycles use the concentrations at the end of the previous run. For the purpose of model evaluation, the

Author's personal copy

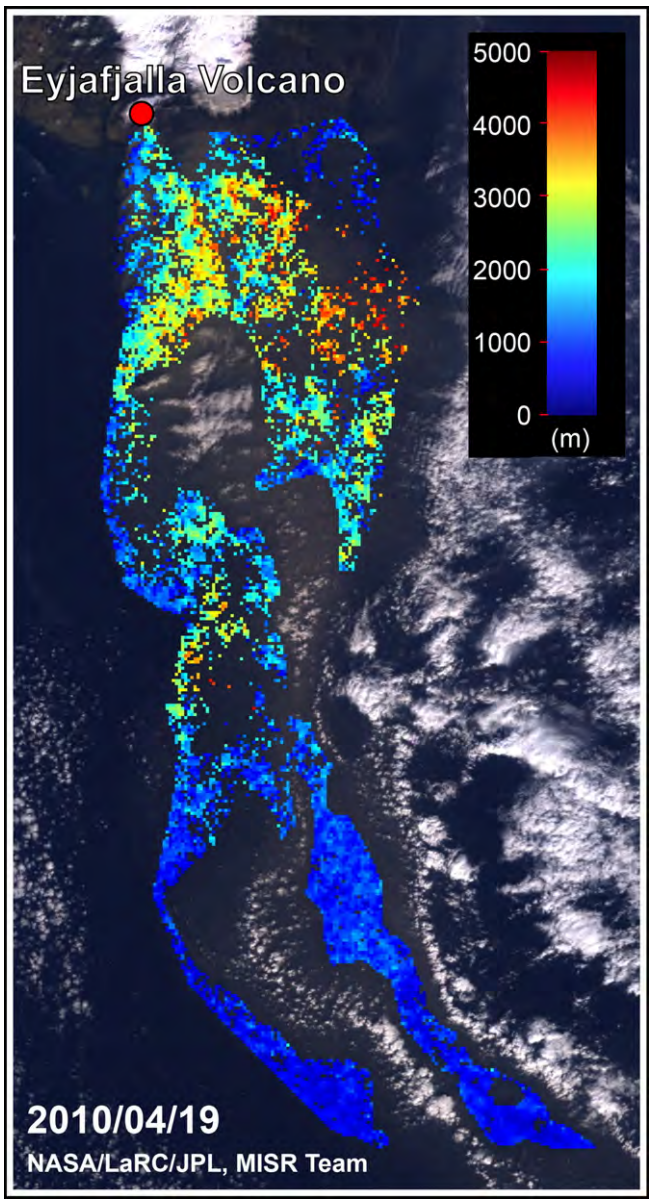

Fig. 3. Volcanic ash plume heights derived from MISR satellite observations on 19 April 2010 (Source: http://www-misr.jpl.nasa.gov).

modelled size-resolved concentration of volcanic ash is converted to aerosol optical thicknesses at 440 nm and 550 nm wavelength as well as vertical profiles of particle backscatter coefficients at 532 nm. The wavelength-dependent particle extinction coefficient is given by:

$$\alpha_k(\lambda) = \sum_i \frac{3Q_{\mathrm{ext}}(\lambda, r_i)C_{i,k}}{4r_i\rho},$$

where Q_{ext} is the dimensionless specific particle extinction efficiency depending on wavelength λ and the effective radius r_i of size fraction i. ρ is the particle density (2650 kg m^{-3}) and $C_{i,\,k}$ denotes the size-resolved aerosol concentration at the model level k with depth Δz_k. Then, the aerosol optical thickness $\tau(\lambda)$ and the backscatter coefficient $\beta_k(\lambda)$ are computed as:

$$\tau(\lambda) = \sum_k \alpha_k(\lambda)\Delta z_k \text{ and}$$

Table 2
Release rates as distributed over six model layers below plume top. The injection heights are given at layer centre and, as an example, for the 19 April 2010.

#	Injection height [km]	Mass fraction [%]
1	3.00	3
2	2.75	9
3	2.40	22
4	2.13	36
5	1.87	17
6	1.65	13

$$\beta_k(\lambda) = \frac{\alpha_k(\lambda)}{S}$$

with the extinction-to-backscatter ratio (lidar ratio) S. Since the ash particle mixture consisting of volcanic glass, minerals, and lithic fragments shows similar light absorption properties like Saharan dust, the extinction efficiency at $\lambda = 440$ nm is calculated from Mie theory using dust refractive indices from Sokolik and Toon (1996) and is 1.684 for the smallest size bin, 3.165, 2.352, 2.145, and 2.071 for the larger bins. A lidar ratio of 55 sr is assumed (Ansmann et al., 2010).

3.2. Aerosol measurements

The model results are evaluated with AERONET (Holben et al., 1998) sun photometer measurements of sun and sky radiances. We make use of values of the cloud-screened aerosol optical thickness (AOT) at 440 nm (Level 1.5) from the European stations: Chilbolton (Chi), Cabauw (Cab), Lille (Lil), Arcachon (Arc), Hamburg (Ham), Mainz (Mai), Leipzig (Lei), and Munich (Mun) (see Fig. 4 for the location). Vertical profiles of the 532 nm particle backscatter coefficient are used to validate the vertical structure of the modelled volcanic ash plume. The measurements were performed with the aerosol Raman lidar operated by the Leibniz Institute for Tropospheric Research (IfT) in Leipzig (Ansmann et al., 2010, 2011). The uncertainties of the backscatter coefficient range from 5% to 10% in the case of dense volcanic plumes, and the uncertainty in AOT measurements is <0.03 (Ansmann et al., 2011, and references therein). In addition, near-surface measurements of PM10 particle mass concentrations are taken from four German atmospheric observation sites: Schauinsland (UBA – German Federal Environment Agency), Zugspitze (UBA), Hohenpeissenberg (DWD), and Melpitz (IfT). Aerosol observation data from the four sites are pooled by the German Ultrafine Aerosol Network (GUAN; Birmili et al., 2009). Zugspitze and Hohenpeissenberg also form a double-site Global Atmosphere Watch station. For a detailed description of the Melpitz site, see Spindler et al. (2010). The PM10 data shown in this work also appear in a more detailed study (Schäfer et al., 2011), which is concerned with the effect of the Eyjafjallajökull volcanic eruption on the surface air quality in the entire south German region. The measurement uncertainty for PM10 is estimated to be 10%. The particle mass concentrations are computed from particle size distribution measurements of various aerosol species assuming a bulk density of 1600 kg m^{-3}. It has to be kept in mind for model evaluation that this value is lower than the density assumed for ash particles.

4. Results

4.1. The modelled Eyjafjallajökull ash plume over Europe

Maps of modelled volcanic ash AOT at 500 nm are shown in Figs. 4 and 5 to illustrate dispersion and evolution of the Eyjafjallajökull ash plume over Europe for selected episodes in April and

Author's personal copy

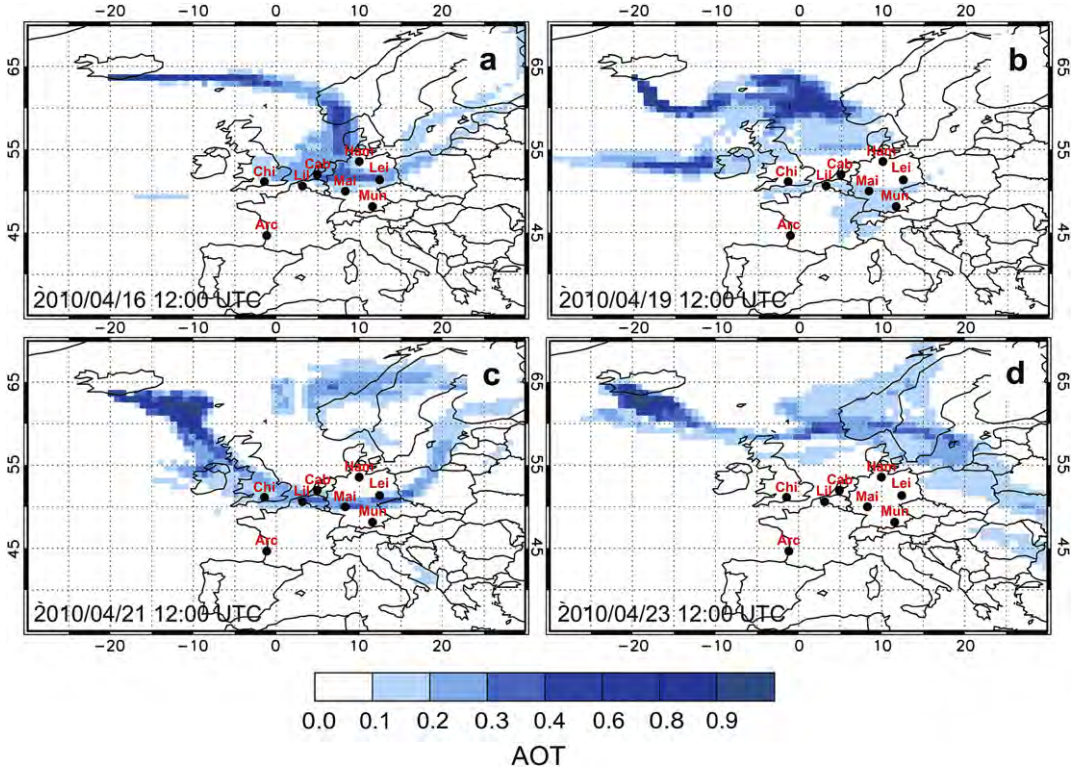

Fig. 4. Maps of model-derived aerosol optical thickness (550 nm) of the Eyjafjallajökull ash plume on 16, 19, 21 and 23 April 2010. Black dots mark the location of AERONET sun photometer stations.

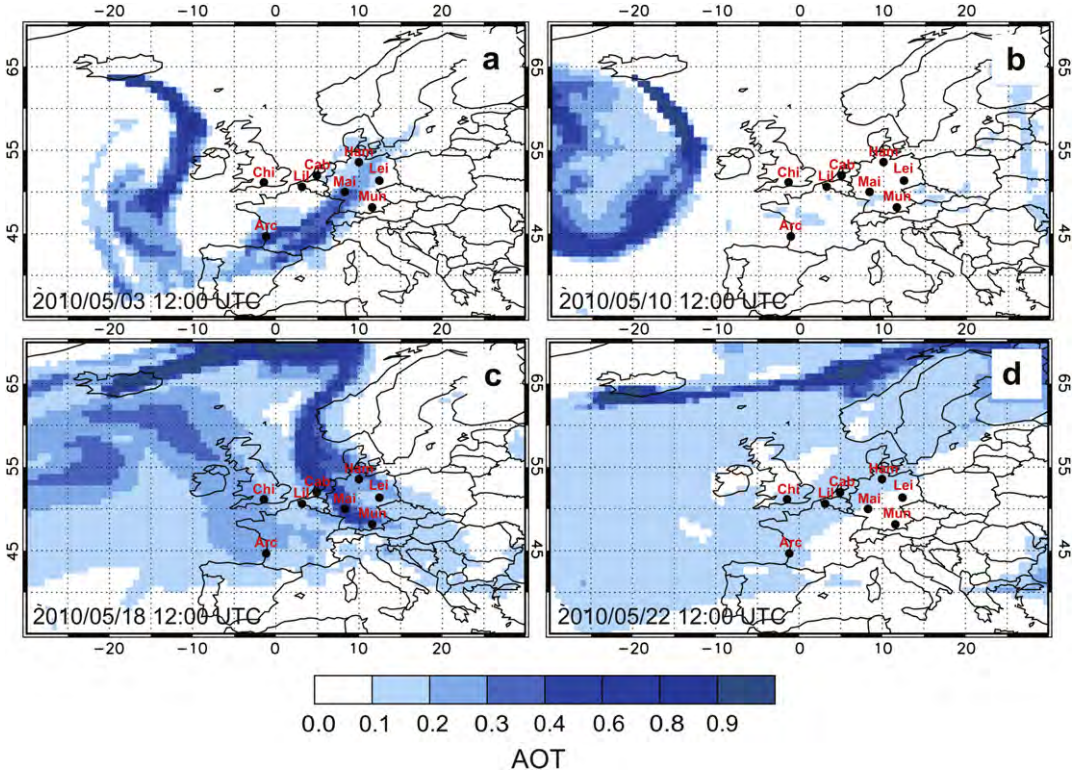

Fig. 5. Same as Fig. 4 but for 3, 10, 18 and 22 May 2010.

Author's personal copy

May 2010. During the first phase of eruptions of the Icelandic volcano from 14 to 17 April a thick ash plume was ejected into the troposphere reaching heights of 9–10 km. A persistent high-pressure system over and to the west of the British Isles and a low-pressure system over Scandinavia controlled the weather conditions during this time period. As a consequence, the volcanic aerosol mass was effectively transported from Iceland towards Central Europe until 16 April (Fig. 4a). Within the following days, major parts of Western Europe were covered by the aerosol plume, which a second time crossed southern Germany on 19–20 April (Fig. 4b). On 19 April, the eruptions began to intensify again. The freshly emitted volcanic aerosol was transported along the northern flank of a high-pressure zone extending from Greenland to Greece in south-westerly direction and reached Germany on 21 April. A part of volcanic ash was advected in a cyclonic motion around the Scandinavian low (Fig. 4c). The transport path shifted northwards on the next days, so that Scandinavia, the Baltic Sea and Eastern Europe were affected by the volcanic ash plume while Western Europe remained clear (Fig. 4d). In the beginning of May the volcanic activity and ash production started once more. However, the weather conditions had changed to an intense high-pressure zone over the northern Atlantic Ocean and a deep trough spanning the British Isles, the North Sea and northern parts of the European continent. The Eyjafjallajökull ash plume spread over the Atlantic Ocean and reached Germany from southwest via the Iberian Peninsula and France on 3 May 2010 (see Fig. 5a). Around 10 May the trough deepened with a low-pressure system over the Biscay whereby ash aerosol was advected around the surface high over the Atlantic Ocean and the transport towards Europe stopped. Only remnants of previous ash plumes left over the continent (Fig. 5b). Again, the eruptions intensified in the middle of May. Central Europe was significantly influenced by volcanic ash on 17–18 April (Fig. 5c). The activity of the Eyjafjallajökull volcano finally ceased on 21–22 May (Table 1, Fig. 5d).

4.2. Comparison of model results to observations

4.2.1. Volcanic ash optical thickness

Fig. 6 shows the temporal evolution of the Icelandic volcano ash AOT over Europe at several AERONET sun photometer stations. The measurements are compared to model-derived values of AOT at 440 nm. When the ash front reached the continent from the eastern North Sea, optical thicknesses of up to 1.4 were observed at Hamburg in the morning on 16 April (Fig. 6e). During further west- and southward transport of the plume, the AOT increased up to 0.6 in Cabauw and Leipzig (Fig. 6a, f). At Chilbolton and Lille maximum values of 0.5 and 0.7 were reported for this day, respectively (Fig. 6b, c). The AOT measurements at Munich in southern Germany reached up to 0.9 on the morning of 17 April (Fig. 6h). The station Arcachon on the western Atlantic coast of France remained unaffected in April 2010. However, within a new phase of volcanic activity around 1 May 2010, the volcanic plume was transported across the Atlantic Ocean and the Iberian Peninsula and caused an increase in AOT to 0.4–0.9 also at Arcachon on the following days (Fig. 6d). The sun photometer measurements indicate that mainly Cabauw, Hamburg, Lille and Mainz were affected by the last intensification of eruptions in mid-May (Fig. 6a,e,c). The AOT reached values of 0.5–1.5 at these stations from 15 to 20 May. The model reproduces the temporal evolution of the AOT of volcanic ash well at the beginning and the end of the eruption period. Nevertheless, some AOT peaks caused by the passage of sharp ash fronts are significantly overestimated in the model. At the German AERONET stations Leipzig, Mainz and Munich the AOT on 19 and 20 April remains at values of only 0.25–0.4 in the model results (Fig. 6f, g, h). This underestimation is possibly related to incorrect emission parameters, but can also be explained by the fact that the model only accounts for primary particle transport, while the aerosol conditions during this time period were determined by the secondary formation of sulphate particles within aged volcanic ash plumes (Ansmann et al., 2011). Moreover, the sun photometer measurements indicate generally high ash concentrations on 25–30 April, which is not confirmed by the model except for Leipzig and Hamburg (Fig. 6f, e). Also in this case, volcanic sulphate particles were probably responsible for the increased aerosol load over Europe, since the activity of the Eyjafjallajökull was in fact low during this phase (Table 1).

4.2.2. Ground-level volcanic aerosol concentration

In addition, volcanic aerosol particles were measured at several German air quality stations. The observed PM10 concentrations are compared with the modelled ash concentrations at Schauinsland, Melpitz, Zugspitze and Hohenpeissenberg for the period 15–23 April 2010 in Fig. 7. There are two aspects to keep in mind for model evaluation. On one hand, the measurements include background aerosol and ash particle mass, so that the model results are expected to be lower than the observations. On the other hand, the observed ash-related aerosol mass could be up to two-third higher assuming the ash particle density of 2650 kg m^{-3}, which is used in the model, instead of 1600 kg m^{-3} assumed for the air quality measurements. At the Schauinsland site (1205 m asl) located in the Black Forest the particle concentrations temporarily increased to about 140 μg m^{-3} in the evening on 17 April probably due to downward mixing of volcanic aerosol. Then, the values continuously increased from the background at 25 μg m^{-3} reaching a maximum of about 150 μg m^{-3} on 19 April 2010. During the next day there was a considerable decrease before the particle concentrations slightly increased again on 21 April. Despite the uncertainties in the assumption of emission parameters and the fact that volcanic sulphate particles are not considered in the model simulations, a good agreement is found between observations and model results. However, the model significantly overestimates the ash particle concentration from the 21 April at around 12:00 UTC. Surface concentrations of PM10 of up to 50 μg m^{-3} were recorded at Melpitz (87 m asl) on 19 and 21 April. The model computes an unrealistically high ash particle concentration of more than 200 μg m^{-3} at surface during the passage of the sharp ash front on 16 April. For the remaining period, the model results are within the range of aerosol measurements, but the modelled temporal evolution hardly agrees with the observations. At the Zugspitze station (2650 m asl), a maximum surface concentration of 60 μg m^{-3} was reached under volcanic aerosol conditions in the night of 17–18 April and in the evening on 19 April. Similar values were reported for the Hohenpeissenberg (977 m asl), only the temporal change was slightly different with a more gradual increase in the beginning. The times at which the maximum surface concentrations are simulated match the observations reasonably well. The model results are almost identical at both locations. The two stations are situated at different orographic heights but at similar longitudes. Difficulties may exist to resolve the differences in the surface ash concentration resulting from different orographic conditions. Generally, the modelled values are too high by a factor of 2–3 at these air quality stations with maximum mass concentrations of up to 170 μg m^{-3}. This mismatch between model results and measurements can be caused by a vertical misplacement of the ash plume or a too strong downward mixing of ash particles from free-tropospheric layers. An overestimation of the volcanic emissions is unlikely, since at Schauinsland and Melpitz, the order of magnitude is consistent with the observations.

Author's personal copy

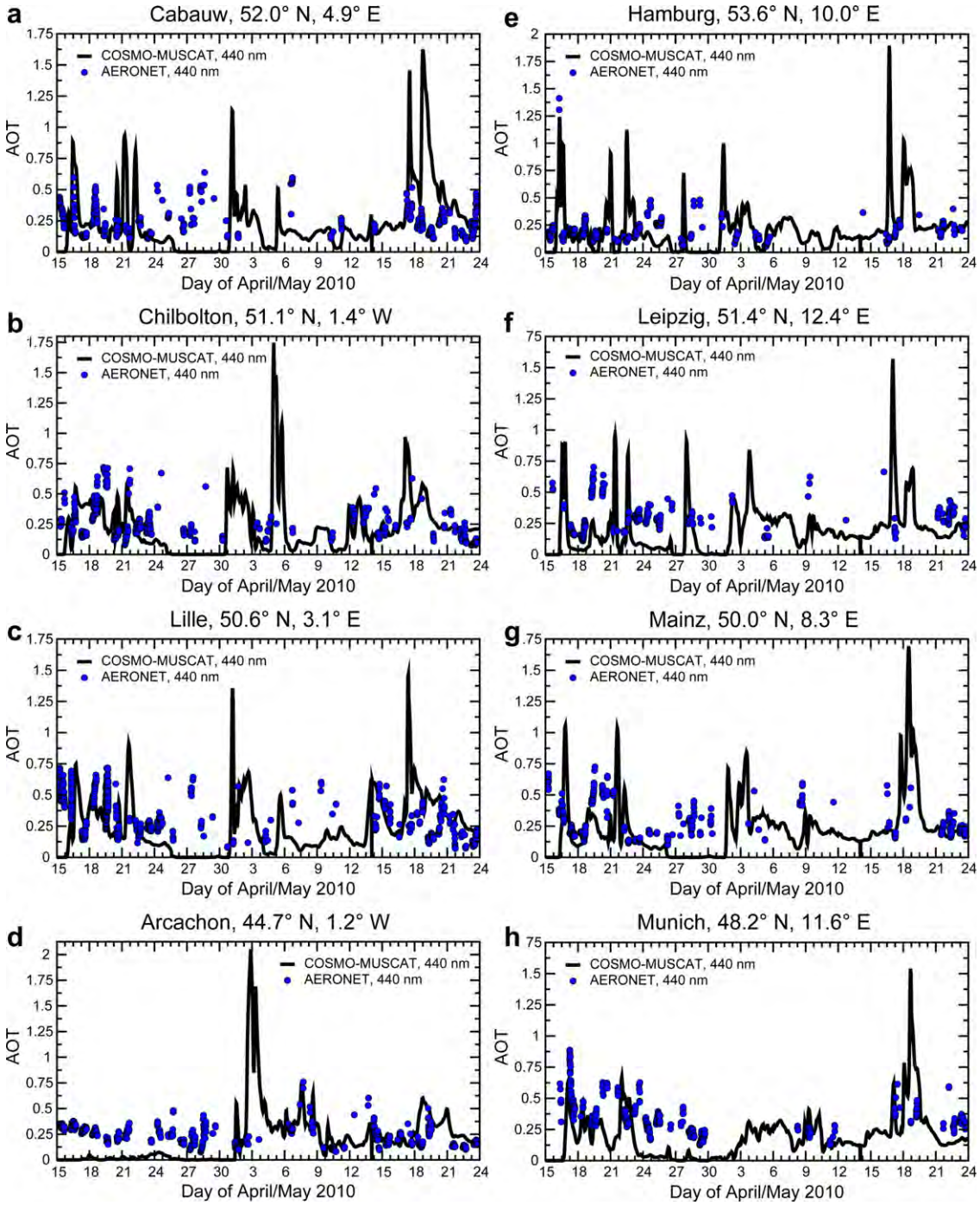

Fig. 6. Aerosol optical thickness (440 nm) at Cabauw, Chilbolton, Lille, Arcachon, Hamburg, Leipzig, Mainz and Munich on 15 April–24 May 2010. Comparison between AERONET sun photometer measurements and model-derived aerosol optical thicknesses. AOT values larger than 0.75 measured after 16/17 April 2010 were most likely related to cirrus clouds, and thus are not shown.

4.2.3. Vertical profiles of volcanic ash

Fig. 8a and b show the vertical distribution of the volcanic ash plume over Leipzig on 16 and 19 April 2010. Profiles of the 532-nm backscatter coefficient from lidar measurements reveal the presence of volcanic ash at 4.5–6 km height at around 12:30 UTC on 16 April. The observed backscatter coefficients reached up to 6 Mm^{-1} sr^{-1} within this plume. Another dense ash layer was centred at 3 km above ground-level (agl) (Fig. 8a). As surface microphysical measurements at Melpitz (see Fig. 7b) suggest, ash particles most likely also contributed to the boundary layer aerosol in the lowest 1.5 km over Leipzig on 16 April. The model matches the vertical profile of volcanic ash very well, even though the fine layer structure is not resolved in the free troposphere. The model-derived backscatter coefficients show a second peak of up to 3 Mm^{-1} sr^{-1} at about 1 km height indicating that ash aerosol mass was mixed down to surface layers (Fig. 8a). During the next days, the ash plume subsided when staying over Western Europe. On 19 April the aged volcanic ash plume returned and crossed Leipzig a second time between 1.5 and 3 km agl

Author's personal copy

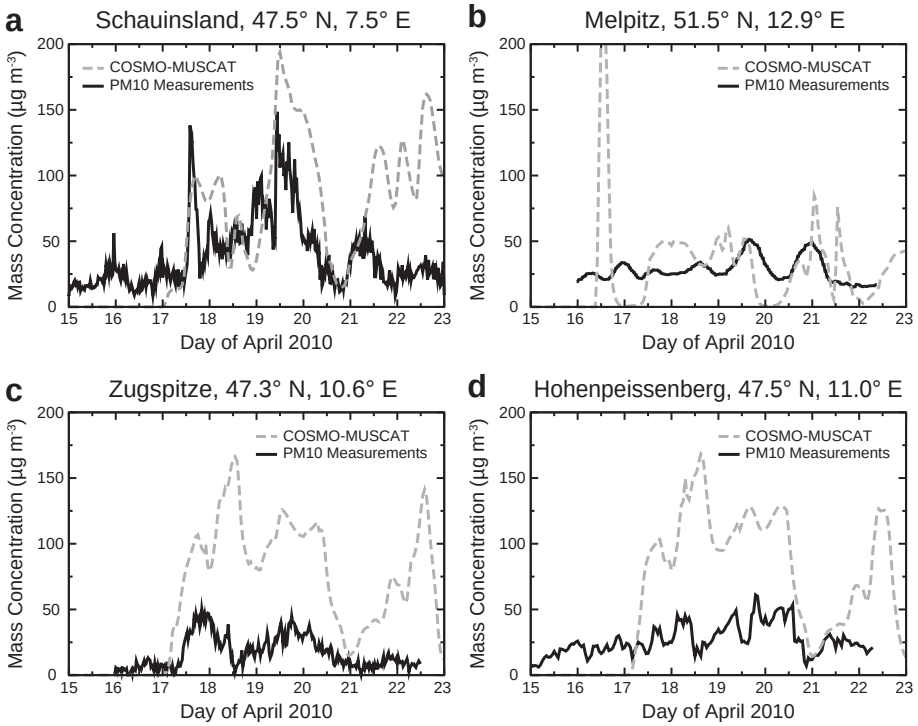

Fig. 7. Comparison between observed and modelled surface mass concentrations of PM10 at Schauinsland, Melpitz, Zugspitze and Hohenpeissenberg on 15–23 April 2010. Source of experimental data: UBA, IfT and DWD (Schäfer et al., 2011).

(Fig. 8b). A maximum backscatter coefficient of 2.3 Mm^{-1} sr^{-1} was found at about 2.4 km height, above which the ash concentration declined rapidly. The maximum of backscatter coefficients is correctly placed by the model. However, the propagation of the modelled ash front is delayed. A good agreement is found when the mean lidar profile from 03:30 UTC–04:23 UTC is compared to the model results for 05:00 UTC (Fig. 8b).

4.3. Impact of the injection height

The sensitivity of the modelled volcanic aerosol transport to different release heights is investigated by simulating the dispersion of additional ash particle tracers. These are emitted in model layers below (in Figs. 8a and 9 referred to as "Low"), within ("Medium") and above ("High") the standard emission height range ("MISR"). Figs. 8a

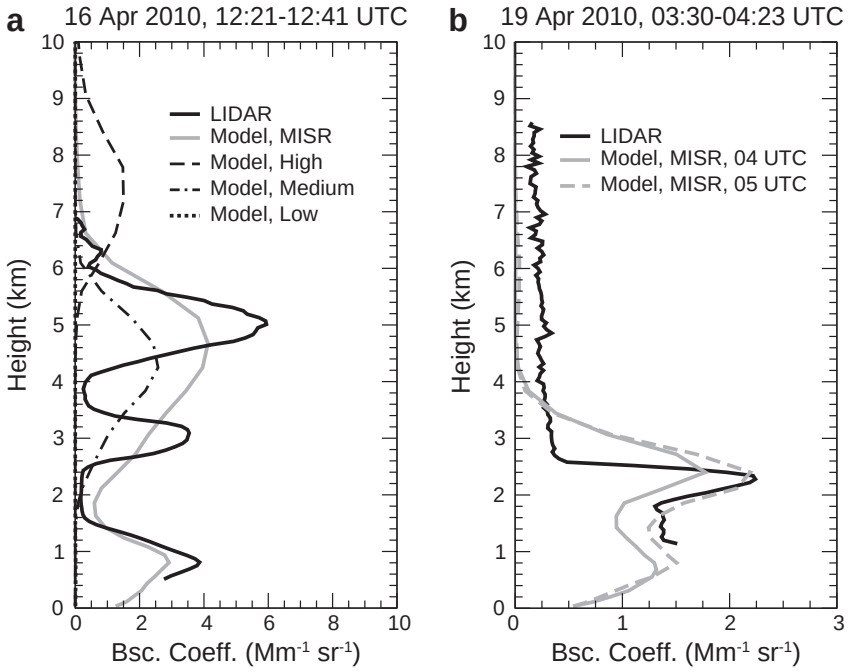

Fig. 8. Vertical profiles of the particle backscatter coefficient (532 nm) over Leipzig on 16 and 19 April 2010. Comparison of modelled profiles with lidar data. The lidar signal profiles measured from 12:21–12:41 UTC on 16 April 2010 and from 03:30–4:23 UTC on 19 April are averaged. The dashed/dotted lines in (a) denote model results with different injection heights.

Author's personal copy

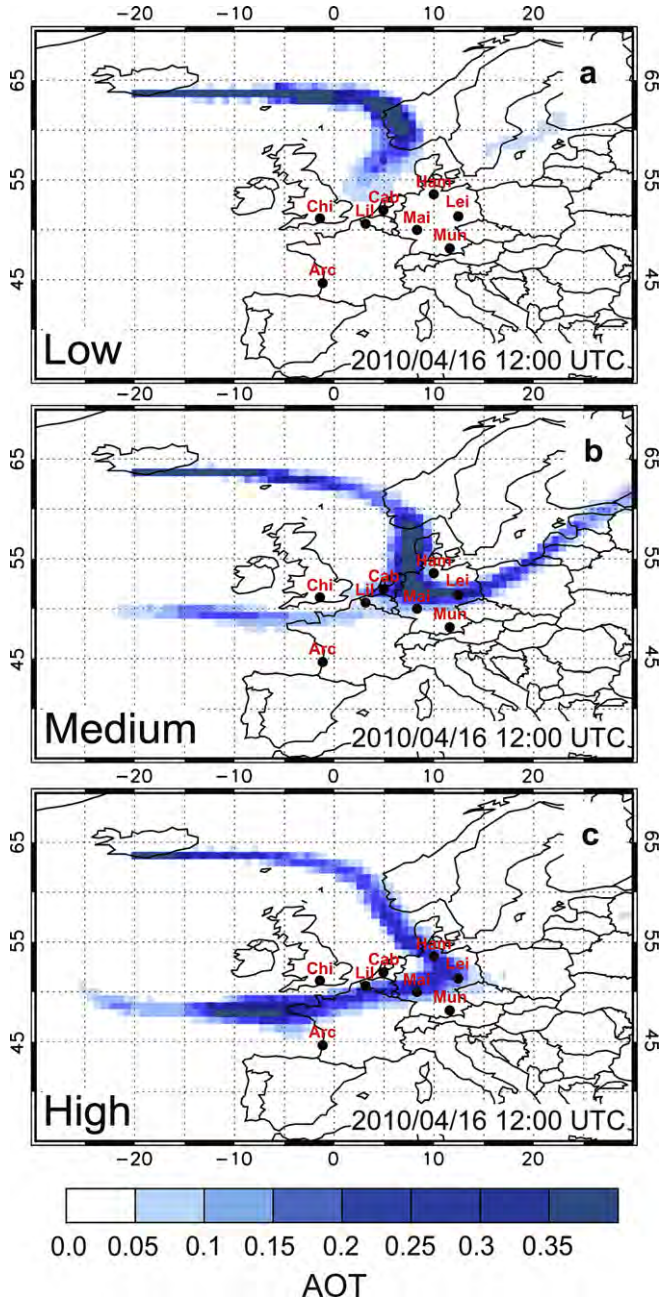

Fig. 9. Maps of aerosol optical thickness on 16 April 2010 showing the variability in the volcanic ash dispersal as computed with COSMO–MUSCAT using different injection heights.

and 9 illustrate for the 16 April, how the spatial distribution of the ash plumes varies with the model vertical level at which they are released. The lower part of the Eyjafjallajökull ash plume quickly subsides and reaches only the North Sea, while the middle part is transported across the European continent and towards the Atlantic Ocean. This corresponds most to the "MISR" standard case. Volcanic ash, which is emitted above the plume top height from London VAAC reports and MISR satellite retrievals, mainly moves clockwise around the high-pressure system east of the British Isles and is advected over the Atlantic Ocean. In Fig. 8a the model-derived backscatter coefficients of volcanic ash from the different injection heights are compared to the lidar observations at Leipzig on 16 April. Volcanic aerosol released below the standard injection height does not arrive at Leipzig. The observed plume height is slightly underestimated in the "Medium" case. However, the plume is placed too high at 7–8 km for the highest emission heights. The comparison reveals that a combination of the injection heights of the "Medium" and "High" case represents the actual spatial–temporal evolution of the Eyjafjallajökull ash plume. This finding confirms the assumptions made in the "MISR" standard case.

5. Summary and discussion

The spread of the volcanic plume from the eruption of the Eyjafjallajökull volcano on Iceland in April and May 2010 was investigated by dispersion simulations with the regional aerosol transport model COSMO–MUSCAT. For model initialisation we used early estimates of primary PM10 emissions, which were obtained from field observations within 72 h after the start of the eruptions. COSMO–MUSCAT allows for a size-resolved description of the spatial and temporal plume evolution. The initial size spectrum was obtained by adapting to in-situ measurements taken during a DLR research flight within the volcanic ash layer over Germany. London VAAC reports on plume top heights as well as statistics on the vertical extent of the Eyjafjallajökull plume provided by the MISR plume height project allowed to setup maximum injection heights and to apply vertically resolved emission rates.

The model results were evaluated using sun photometer measurements from the European AERONET stations, lidar observations at Leipzig and ground-level microphysical measurements at selected air quality stations in Germany. A good agreement was found regarding the magnitude and temporal evolution of the volcanic ash AOT, except for the middle of the eruption period, when the modelled values of AOT were mainly too low. There were several unrealistically high AOT peaks in the model results related to the passage of sharp ash fronts. The comparisons with PM10 concentrations from ground-based measurements indicate that the model was able to reasonably reproduce the volcanic aerosol mass near the surface at two of the four sites. Also the vertical distribution of the Eyjafjallajökull plume was matched by the model. Measured and modelled profiles of the ash particle backscatter coefficient agreed very well with respect to the plume height and the magnitude of the values.

Discrepancies between model and observations mostly resulted from the uncertainties in the eruption emission parameters (i.e., emission rate, injection height, distribution of ash release with altitude and particle size distribution) and modelled wind fields. In addition, underestimations of the simulated volcanic aerosol mass occurred, since only primary ash particles were considered by the model, while observations indicated a considerable contribution of secondary volcanic sulphate particles to the aerosol load over Europe. A general validation problem is due to the fact that local measurements, which represent the conditions at one point, may not be representative of an entire model grid cell. This is in particular relevant for the narrow ash plumes that passed the continent during the volcano eruption period. Moreover, the comparability of model results and measurements of AOT and lidar backscatter coefficients is sensitive to the assumption of optical particle properties (i.e., extinction efficiency and lidar ratio).

The impact of the injection height on the dispersion and evolution of the volcanic ash plume over Europe was investigated. Additional ash tracers were emitted at control levels below, within and above the standard emission height range, and their transport paths were tracked independently. The comparison of modelled vertical profiles of ash backscatter coefficients to lidar measurements showed how the different injection heights contributed to the actual ash plume of the Eyjafjallajökull volcano. Independently of the evaluation with observations, these results confirm the assumptions made in the standard case using MISR plume height retrievals.

Author's personal copy

Taking into account the remaining uncertainties listed above, COSMO–MUSCAT performed well in simulating the 2010 Icelandic volcano ash plume. The model capability to reproduce the vertical profiles of volcanic ash showed that the MISR stereo-height retrievals are suitable to initialise vertically resolved emissions of volcanic ash in aerosol transport simulations. They are an alternative to complex injection height models, when information on eruption dynamics is unavailable. Applications like this should encourage the team of the MISR plume height project to further build up their data base for other cases of deep aerosol plumes.

Acknowledgements

The eruption emission parameters used in this study were compiled and distributed by The Norwegian Meteorological Institute. The authors are grateful to NASA's MISR team for the production and distribution of height retrievals for the Icelandic volcano eruption. We thank C.L. Wrench, G. de Leeuw, P. Goloub, N. Martiny, S. Kinne, M. Andreae, and P. Koepke for kindly providing AERONET data. PM10 data were kindly provided by G. Spindler (IfT), L. Ries (UBA, GAW station Zugspitze), F. Meinhardt (UBA, Schauinsland), and H. Flentje (DWD, MOHp Hohenpeissenberg). We also acknowledge good cooperation and support from the Deutscher Wetterdienst (DWD, Offenbach) and the John von Neumann Institute for Computing (Jülich).

References

Ansmann, A., Tesche, M., Groß, S., Freudenthaler, V., Seifert, P., Hiebsch, A., Schmidt, J., Wandinger, U., Mattis, I., Wiegener, M., 2010. The 16 April 2010 major volcanic ash plume over central Europe: EARLINET lidar and AERONET photometer observations at Leipzig and Munich, Germany. Geophysical Research Letters 37, L13810. doi:10.1029/2010GL043809.

Ansmann, A., Tesche, M., Seifert, P., Groß, S., Freudenthaler, V., Apituley, A., Wilson, K.M., Serikov, I., Linné, H., Heinold, B., Hiebsch, A., Schnell, F., Schmidt, J., Mattis, I., Wandinger, U., Wiegner, M., 2011. Ash and fine-mode particle mass profiles from EARLINET-AERONET observations over central Europe after the eruptions of the Eyjafjallajokull volcano in 2010. Journal of Geophysical Research. doi:10.1029/2010JD015567.

Berge, E., 1997. Transboundary air pollution in Europe. In: MSC-W Status Report 1997, Part 1 and 2. The Norwegian Meteorological Institute, Oslo EMEP/MSC-W Report 1/97.

Birmili, W., Weinhold, K., Nordmann, S., Wiedensohler, A., Spindler, G., Müller, K., Herrmann, H., Gnauk, T., Pitz, M., Cyrys, J., Flentje, H., Nickel, C., Kuhlbusch, T.A.J., Löschau, G., Haase, D., Meinhardt, F., Schwerin, A., Ries, L., Wirtz, K., 2009. Atmospheric aerosol measurements in the German Ultrafine Aerosol Network (GUAN): part 1-soot and particle number size distributions. Gefahrstoffe Reinhaltung der Luft 69 (4), 137–145.

Casadevall, T.J., 1994. The 1989–1990 eruption of Redoubt Volcano, Alaska: impacts on aircraft operations. Journal of Volcanology and Geothermal Research 62, 301–316.

Flentje, H., Claude, H., Elste, T., Gilge, S., Köhler, U., Plass-Dülmer, C., Steinbrecht, W., Thomas, W., Werner, A., Fricke, W., 2010. The Eyjafjallajökull eruption in April 2010 – detection of volcanic plume using in-situ measurements, ozone sondes and lidar-ceilometer profiles. Atmospheric Chemistry and Physics 10, 10085–10092. doi:10.5194/acp-10-10085-2010.

Gudmunsson, M.T., Pedersen, R., Vogfjörd, K., Thorbjarnardottir, B., Jakobsdottir, S., Roberts, M.J., 2010. Eruptions of the Eyjafjallajökull volcano, Iceland. EOS 91 (21), 190–191.

Heinold, B., Helmert, J., Hellmuth, O., Wolke, R., Ansmann, A., Marticorena, B., Laurent, B., Tegen, I., 2007. Regional modeling of Saharan dust events using LM-MUSCAT: model description and case studies. Journal of Geophysical Research 112, D11204. doi:10.1029/2006JD007443.

Heinold, B., Tegen, I., Esselborn, M., Kandler, K., Knippertz, P., Müller, D., Schladitz, A., Tesche, M., Weinzierl, B., Ansmann, A., Althausen, D., Laurent, B., Maßling, A., Müller, T., Petzold, A., Schepanski, K., Wiedensohler, A., 2009. Regional Saharan dust modelling during the SAMUM 2006 campaign. Tellus 61B. doi:10.1111/j.1600-0889.2008.00387.x.

Holben, B.N., Eck, T.F., Slutsker, I., Tanre, D., Buis, J.P., Setzer, A., Vermote, E., Reagan, J.A., Kaufman, Y., Nakajima, T., Lavenu, F., Jankowiak, I., Smirnov, A., 1998. AERONET – A federated instrument network and data archive for aerosol characterization. Remote Sensing of Environment 66, 1–16.

Jones, A., Johnson, D., Hort, M., Devenish, B., 2007. The UK met office's next-generation atmospheric dispersion model, NAME III. In: Borrego, C., Norman, A.-L. (Eds.), Air Pollution Modeling and Its Application XVII. Springer, pp. 580–589. doi:10.1007/978-0-387-68854-1.

Kahn, R.A., Li, W.H., Moroney, C., Diner, D.J., Martonchik, J.V., Fishbein, E., 2007. Aerosol source plume physical characteristics from space-based multiangle imaging. Journal of Geophysical Research 112, D11205. doi:10.1029/2006JD007647.

Miller, T., Casadevall, T., 2000. Encyclopedia of Volcanoes, Chapter: Volcanic Ash Hazards to Aviation. Elsevier, New York, pp. 915–930.

Renner, E., Wolke, R., 2010. Modelling the formation and atmospheric transport of secondary inorganic aerosols with special attention to regions with high ammonia emissions. Atmospheric Environment 44 (15), 1904–1912. doi:10.1016/j.atmosenv.2010.02.018.

Schäfer, K., Thomas, W., Peters, A., Ries, L., Obleitner, F., Schnelle-Kreis, J., Birmili, W., Diemer, J., Fricke, W., Junkermann, W., Pitz, M., Emeis, S., Forkel, R., Suppan, P., Flentje, H., Wichmann, H.E., Gilge, S., Meinhardt, F., Zimmermann, R., Weinhold, K., Soentgen, J., Münkel, C., Freuer, C., Cyrys, J., 2011. Influences of the 2010 Eyjafjallajökull volcanic plume on air quality in the northern Alpine region. Atmospheric Chemistry and Physics Discussion 11, 9083–9132. doi:10.5194/acpd-11-9083-2011.

Schumann, U., Weinzierl, B., Reitebuch, O., Schlager, H., Minikin, A., Forster, C., Baumann, R., Sailer, T., Graf, K., Mannstein, H., Voigt, C., Rahm, S., Simmet, R., Scheibe, M., Lichtenstern, M., Stock, P., Rüba, H., Schäuble, D., Tafferner, A., Rautenhaus, M., Gerz, T., Ziereis, H., Krautstrunk, M., Mallaun, C., Gayet, J.-F., Lieke, K., Kandler, K., Ebert, M., Weinbruch, S., Stohl, A., Gasteiger, J., Groß, S., Freudenthaler, V., Wiegner, M., Ansmann, A., Tesche, M., Olafsson, H., Sturm, K., 2011. Airborne observations of the Eyjafjalla volcano ash cloud over Europe during air space closure in April and May 2010. Atmospheric Chemistry and Physics 11, 2245–2279. doi:10.5194/acp-11-2245-2011.

Seinfeld, J.H., Pandis, S.N., 1998. Atmospheric Chemistry and Physics. John Wiley & Sons, New York, pp. 1326.

Scollo, S., Folch, A., Coltelli, M., Realmuto, V.J., 2010. Three-dimensional volcanic aerosol dispersal: a comparison between Multiangle Imaging Spectroradiometer (MISR) data and numerical simulations. Journal of Geophysical Research 115, D24210. doi:10.1029/2009JD013162.

Sokolik, I.N., Toon, O.B., 1996. Direct radiative forcing by anthropogenic airborne mineral aerosols. Nature 381, 681–683.

Spindler, G., Brüggemann, E., Gnauk, T., Grüner, A., Müller, K., Herrmann, H., 2010. A four-year size-segregated characterization study of particles PM10, PM2.5 and PM1 depending on air mass origin at Melpitz. Atmospheric Environment 44, 164–173.

Steppeler, J., Doms, G., Schättler, U., Bitzer, H.W., Gassmann, A., Damrath, U., Gregoric, G., 2003. Meso-gamma scale forecasts using the nonhydrostatic model LM. Meteorology and Atmospheric Physics 107 (D21), 75–96. doi:10.1007/s00703-001-0592-9. 4576.

Weinzierl, B., Petzold, A., Esselborn, M., Wirth, M., Rasp, K., Kandler, K., Schütz, L., Köpke, P., Fiebig, M., 2009. Airborne measurements of dust layer properties, particle size distribution and mixing state of Saharan dust during SAMUM 2006. Tellus 61B, 96–117. doi:10.1111/j.1600-0889.2008.00392.x.

Wolke, R., Knoth, O., 2000. Implicit–explicit Runge–Kutta methods applied to atmospheric chemistry-transport modelling. Environmental Modelling & Software 15, 711–719.

Wolke, R., Hellmuth, O., Knoth, O., Schröder, W., Heinrich, B., Renner, E., 2004. The chemistry-transport modeling system LM-MUSCAT: description and CityDelta applications. In: Borrego, C., Incecik, S. (Eds.), Proceedings of Twenty-sixth NATO/CCMS International Technical Meeting on Air Pollution Modeling and Its Application. Air Pollution Modeling and Its Application, Vol. XVI. Kluwer Academic/Plenum Publishers, New York.